The Plant Cell, Vol. 21: 2655–2671, September 2009, www.plantcell.org

Cellular Pathways Regulating Responses to Compatible and Self-Incompatible Pollen in *Brassica* and *Arabidopsis* Stigmas Intersect at Exo70A1, a Putative Component of the Exocyst Complex [W]

Marcus A. Samuel,[a,1] Yolanda T. Chong,[a,2,3] Katrina E. Haasen,[a,3] May Grace Aldea-Brydges,[a] Sophia L. Stone,[a,4] and Daphne R. Goring[a,b,5]

[a] Department of Cell and Systems Biology, University of Toronto, Toronto, Canada M5S 3B2
[b] Centre for the Analysis of Genome Evolution and Function, University of Toronto, Toronto, Canada M5S 3B2

In the *Brassicaceae*, compatible pollen–pistil interactions result in pollen adhesion to the stigma, while pollen grains from unrelated plant species are largely ignored. There can also be an additional layer of recognition to prevent self-fertilization, the self-incompatibility response, whereby self pollen grains are distinguished from nonself pollen grains and rejected. This pathway is activated in the stigma and involves the ARM repeat–containing 1 (ARC1) protein, an E3 ubiquitin ligase. In a screen for ARC1-interacting proteins, we have identified *Brassica napus* Exo70A1, a putative component of the exocyst complex that is known to regulate polarized secretion. We show through transgenic studies that loss of Exo70A1 in *Brassica* and *Arabidopsis thaliana* stigmas leads to the rejection of compatible pollen at the same stage as the self-incompatibility response. A red fluorescent protein:Exo70A1 fusion rescues this stigmatic defect in *Arabidopsis* and is found to be mobilized to the plasma membrane concomitant with flowers opening. By contrast, increased expression of Exo70A1 in self-incompatible *Brassica* partially overcomes the self pollen rejection response. Thus, our data show that the Exo70A1 protein functions at the intersection of two cellular pathways, where it is required in the stigma for the acceptance of compatible pollen in both *Brassica* and *Arabidopsis* and is negatively regulated by *Brassica* self-incompatibility.

INTRODUCTION

In many flowering plants, complex pollen–stigma interactions have evolved to allow for the specific recognition of compatible pollen. Species of the crucifer family (e.g., *Brassica napus* and *Arabidopsis thaliana*) have dry stigmas (absence of surface secretions), which prevent pollen grains from unrelated plant species (foreign pollen) from adhering and germinating at the earliest stages of pollination. When compatible pollen comes in contact with the dry stigma, hydraulic connectivity is established to facilitate the passage of water into the pollen grains. Hydrated pollen grains germinate and produce tubes that penetrate the stigmatic cell walls and traverse the pistil down to the ovules where fertilization takes place (Dickinson, 1995; Swanson et al., 2004). Thus, only compatible pollen grains are capable of inducing the stigma to release necessary resources, such as water and other factors, while foreign pollen grains are largely ignored. As a result, plant species with dry stigmas prevent foreign pollen from inappropriately using female resources (Heslop-Harrison, 1981). Genetic screens have identified various compatibility factors in both the pollen and stigma, but the cellular mechanism regulating this recognition process is still poorly understood (Edlund et al., 2004; Hiscock and Allen, 2008).

The pollen exine is required for the initial stage of pollen capture, and the proteins and lipids in the pollen coat promote subsequent stages of interactions (Hulskamp et al., 1995; Zinkl et al., 1999). For example, *Arabidopsis eceriferum* mutants have severely reduced pollen coats and are male sterile (Fiebig et al., 2000). Additionally, the lack of Glycine Rich Protein-17, an oleosin domain protein, was found to cause delayed pollen hydration (Mayfield and Preuss, 2000). The lipids from the pollen coat are proposed to interact with the lipids of the stigmatic cuticle to form a hydraulic conduit for passage of water from the stigma to pollen, thus facilitating pollen hydration. Interestingly, *Arabidopsis* fiddlehead mutants, which possess altered cuticular properties, support pollen hydration on nonstigmatic tissues (Lolle and Cheung, 1993). Another layer of pollen growth is regulated by the stigmatic pellicle, the proteinaceous, outermost layer of the stigmatic papilla that comes in contact with the pollen grain. Removal of the pellicle results in a lack of pollen tube entry into the stigma (Roberts et al., 1984). Two *Brassica* stigmatic proteins, the S-locus related 1 (SLR1) and S-locus glycoprotein (SLG), have been implicated in the early stages of pollen

[1] Current address: Department of Biological Sciences, University of Calgary, Calgary, Canada T2T 1N4.
[2] Current address: Terrence Donnelly Centre for Cellular and Biomedical Research, University of Toronto, Toronto, Canada M5S 3E1.
[3] These authors contributed equally to this work.
[4] Current address: Department of Biology, Dalhousie University, Halifax, Nova Scotia, Canada B3H 4J1.
[5] Address correspondence to d.goring@utoronto.ca.
The author responsible for distribution of materials integral to the findings presented in this article in accordance with the policy described in the Instructions for Authors (www.plantcell.org) is: Daphne R. Goring (d.goring@utoronto.ca).
[W] Online version contains Web-only data.
www.plantcell.org/cgi/doi/10.1105/tpc.109.069740

adhesion. Both the transgenic suppression of SLR-1 and antibody-mediated masking of SLR1 and SLG binding sites resulted in reduced pollen adhesion (Luu et al., 1999). SLR1 and SLG are proposed to mediate adhesion through their binding to the pollen coat proteins, SLR1-BP and PCP-A1, respectively (Doughty et al., 1998; Takayama et al., 2000a).

In addition to the recognition of compatible pollen, the self-incompatibility system may also be present and activated in the stigma following contact with self pollen. In this response, pollen rejection occurs by blocking pollen hydration and the pollen tube penetration through the stigmatic surface (Dickinson, 1995; Hiscock and McInnis, 2003; Takayama and Isogai, 2005). Genetic and molecular studies have elucidated several components involved in *Brassica* self-incompatibility. This response is initiated by the pollen coat protein, S-locus Cys-rich/S-locus protein 11 (SCR/SP11), and the stigma-specific *S* Receptor Kinase (SRK), which are encoded by a pair of tightly linked, multiallelic loci (Schopfer et al., 1999; Takasaki et al., 2000; Takayama et al., 2000b; Silva et al., 2001). Following the attachment of self pollen to the stigma, SCR/SP11 binds to the membrane-localized SRK, and this receptor-ligand interaction activates SRK (Kachroo et al., 2001; Takayama et al., 2001). Along with another plasma membrane–localized kinase, M-locus protein kinase, SRK is proposed to interact with and phosphorylate the E3 ubiquitin ligase, ARM-repeat containing 1 (ARC1), to promote rejection of self pollen (Goring and Walker, 2004; Murase et al., 2004; Kakita et al., 2007). ARC1 exhibits a phosphorylation-mediated interaction with the intracellular domain of SRK and has been shown to have E3 ligase activity (Gu et al., 1998; Stone et al., 2003). The self-incompatibility response has been shown to lead to an increase in ubiquitinated proteins in the *Brassica* stigma, and in *Nicotiana tabacum* BY-2 cells, the activated SRK kinase domain relocalizes ARC1 from the cytosol to the proteasome (Stone et al., 2003). The knocked down expression of ARC1 in self-incompatible *B. napus* W1 lines led to partial breakdown of the self-incompatibility response, and the treatment of W1 pistils with proteasomal inhibitors also resulted in a breakdown of the self-incompatibility response (Stone et al., 2003, 1999). Thus, ARC1 was proposed to be a positive regulator of self-incompatibility, and proteasomal-mediated degradation is thought to be required for the self-incompatibility response to operate. The putative targets of ARC1 were hypothesized to be compatibility factors in the stigma, which are inhibited by the self-incompatibility response, although the identities of the targets of ARC1 were unknown (Stone et al., 2003).

Through a screen for ARC1-interacting proteins, we have now identified a predicted *B. napus* exocyst complex subunit, Exo70A1, as an interactor and substrate for ARC1. In yeast and animal systems, Exo70 is an essential component of the multisubunit exocyst complex, which is involved in targeted secretion at the plasma membrane through the tethering of vesicles on the plasma membrane (Hsu et al., 2004; Munson and Novick, 2006). In both *Brassica* and *Arabidopsis*, the dry stigmas serve as the major source of water, calcium, and other factors necessary for compatible pollen grain hydration and pollen tube penetration through the stigma, indicating a requirement for targeted secretion to pollen attachment sites (Dickinson, 1995). Here, we show that Exo70A1 is a compatibility factor in the stigma and demonstrate that *Brassica* and *Arabidopsis* lines lacking Exo70A1 in the stigma are incapable of accepting compatible pollen. By contrast, overexpression of Exo70A1 in *Brassica* is sufficient to partially overcome the self pollen rejection response in self-incompatible *Brassica* plants. Thus, we present conclusive evidence placing Exo70A1 at the intersection of these two cellular pathways in the stigma.

RESULTS

ARC1 Interacts with and Ubiquitinates Exo70 A1

To identify potential substrates regulated by the ARC1 E3 ligase during the *Brassica* self-incompatibility pathway, a pistil cDNA yeast two-hybrid library was screened and resulted in the isolation of an Exo70 homolog. In plant genomes, there are multiple predicted copies of the *Exo70* gene, and the clone isolated in our study was most similar to the *Arabidopsis Exo70A1* (see Supplemental Figures 1A and 1B online; Synek et al., 2006). The interaction of ARC1 with Exo70A1 was confirmed using in vitro binding assays with recombinant His6:Exo70A1:FLAG and glutathione *S*-transferase (GST):ARC1 fusion proteins (Figure 1). The Exo70A1 fusion protein bound to the Ni beads was able to bind GST:ARC1, and no signal was detected when GST was added (Figure 1A). Similarly, when GST:ARC1 or GST alone were bound to the GSH beads, the His6:Exo70A1:FLAG fusion protein was pulled down only when GST:ARC1 was present (Figure 1B). Since ARC1 has been previously shown to possess E3 ligase activity, we wanted to examine if Exo70A1 can function as a substrate for ARC1. When the His6:Exo70A1:FLAG recombinant protein was added to the ubiquitination assay containing ARC1 (as the E3 enzyme) along with the E1 and E2 enzymes, higher molecular weight laddering, indicative of polyubiquitination, was observed (Figure 1C). In comparison, the control lanes lacking either ARC1 or Exo70A1 did not show this higher molecular weight laddering (Figure 1C). Thus, both the in vitro binding and ubiquitination assays suggest that Exo70A1 can be a binding partner and a substrate for ARC1.

RNA Interference–Mediated Suppression of *Exo70A1* in Compatible Westar Lines Leads to Reduced Pollen Acceptance

The isolation of Exo70A1 as an ARC1 interactor implies a previously unknown role for Exo70 in the stigma during pollen–stigma interactions. ARC1 functions in the stigma as part of the self-incompatibility response and has a positive role promoting the rejection of self pollen. It is predicted to carry out this function by targeting substrate proteins for degradation by the proteasome (Stone et al., 1999, 2003). Following from this, an ARC1 target would be predicted to be required in the stigmatic papillae to accept compatible pollen, and pollen rejection would occur when the target is inactivated. This prediction can be simply tested by removing the target, Exo70A1, from the stigma and testing if compatible pollen can still be accepted. *Brassica Exo70A1* is expressed in several tissues, with highest levels of expression in the pistil and with lowest levels in stamens (Figure

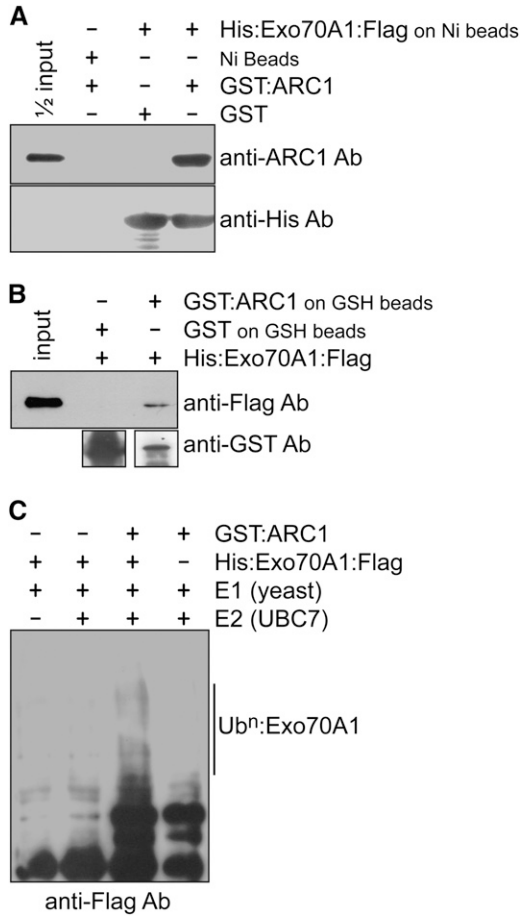

Figure 1. In Vitro Binding and Ubiquitination Assays with *Brassica* ARC1 and Exo70A1.

(A) In vitro binding assay with purified GST or GST:ARC1 added to Ni-NTA–bound His6:Exo70A1:FLAG or Ni-NTA alone. ARC1 binds specifically to Exo70A1.

(B) In vitro binding assay with purified His6:Exo70A1:FLAG protein added to GSH beads bound to GST or GST:ARC1. ARC1 binds specifically to Exo70A1.

(C) In vitro ubiquitination assay of Exo70A1 by the ARC1 E3 ubiquitin ligase. His6:Exo70A1:FLAG was detected using an anti-FLAG antibody. Multi-ubiquitinated Exo70A1 is only detected when all components of the ubiquitination assay are present (lane 3). Due to the long exposure time, some cross-reacting bands from the ARC1 sample are seen at the bottom of the blot in lanes 3 and 4.

2A). Thus, to suppress *B. napus Exo70A1* exclusively in the stigma, the *Exo70A1* RNA interference (RNAi) construct was placed under the control of the stigma-specific SLR1 promoter (Franklin et al., 1996; Stone et al., 1999; Fobis-Loisy et al., 2007), and this construct was transformed into *B. napus* Westar, a fully compatible cultivar that produces full seedpods following self-pollination. Three independent transgenic Westar lines, R1 to R3, were generated and found to have reduced levels of *Exo70A1* in the stigma (Figures 2B and 2C).

As expected, the *Exo70A1* RNAi Westar lines produce flowers of wild-type appearance and viable pollen, with full seedpods observed when wild-type Westar pistils are pollinated with this pollen (Figures 2D and 2E). However, also as predicted, the *Exo70A1* RNAi Westar stigmas are impaired in compatible pollen acceptance, and a corresponding reduction in seed production is observed for all three lines (Figure 2F). The *Exo70A1* RNAi Westar lines pollinated with compatible Westar pollen produced significantly lower means of 5.6 ± 1.6, 3.6 ± 1.4, and 3.2 ± 1.3 seeds/pod compared with 28.4 ± 0.7 seeds/pod produced by the control compatible *B. napus* Westar pollinations (Figure 2G). The self-incompatible *B. napus* W1 line was used as a control for self pollen rejection with the ensuing absence of seed production (Stone et al., 1999, 2003). These results show that *Brassica* Exo70A1 plays an essential role in the stigma during compatible pollen–stigma interactions.

Exo70A1 Overexpression in Self-Incompatible W1 Lines Is Sufficient to Partially Break Down the Self-Incompatibility Response

Based on Exo70A1's essential role in the stigma for compatible pollinations and its ability to interact with and function as a substrate for ARC1, we hypothesized that one way through which ARC1 imparts its E3 ubiquitin ligase activity during self-incompatibility is by targeting Exo70A1 for degradation. If this were true, then elevation of Exo70A1 levels in a self-incompatible line may overcome the pollen rejection response by essentially titrating out ARC1's activity. This prediction was tested by expressing a red fluorescent protein (*RFP*)*:Exo70A1* (*B. napus Exo70A1*) construct under the control of the stigma-specific SLR1 promoter in the self-incompatible *B. napus* W1 line. The *B. napus* W1 line is identified by the presence of the self-incompatibility S_{910} allele through PCR detection of the SRK_{910} gene (Yu et al., 1996; Silva et al., 2001), and two independent transgenic *RFP:Exo70A1* W1 lines, S1 and S2, were generated (Figures 3A and 3B). Consistent with this hypothesis, the S1 and S2 plants had increased seed production following pollination with self-incompatible W1 pollen than did the control self-pollinated W1 plants (Figure 3C). The *RFP:Exo70A1* W1 lines produced averages of 3.4 ± 0.81 and 2.8 ± 0.97 seeds/pods when pollinated with W1 pollen, which was significantly higher than the self-incompatible W1 control, which did not produce any seeds (Figure 3D). All the control compatible pollinations with Westar as the pollen donor for W1, S1, and S2 pistils produced full seedpods, as expected (Figures 3C and 3D). Thus, the increased levels of *Exo70A1* were able to titrate out ARC1's activity and partially overcome the self-incompatibility phenotype of W1 plants.

We attempted to visualize the RFP:Exo70A1 protein in the *B. napus* S1 and S2 lines using confocal microscopy but were unable to detect RFP through the dense *Brassica* stigmatic papillae. The presence of the RFP:Exo70A1 protein in the stigma was confirmed by immunoblot analysis, using an anti-RFP antibody, prior to and after pollination following either W1 and Westar pollinations (see Supplemental Figure 2 online). While activation of the self-incompatibility pathway leading to ARC1-mediated degradation of Exo70A1 would be predicted to reduce Exo70A1 protein levels following W1 pollinations, no clear

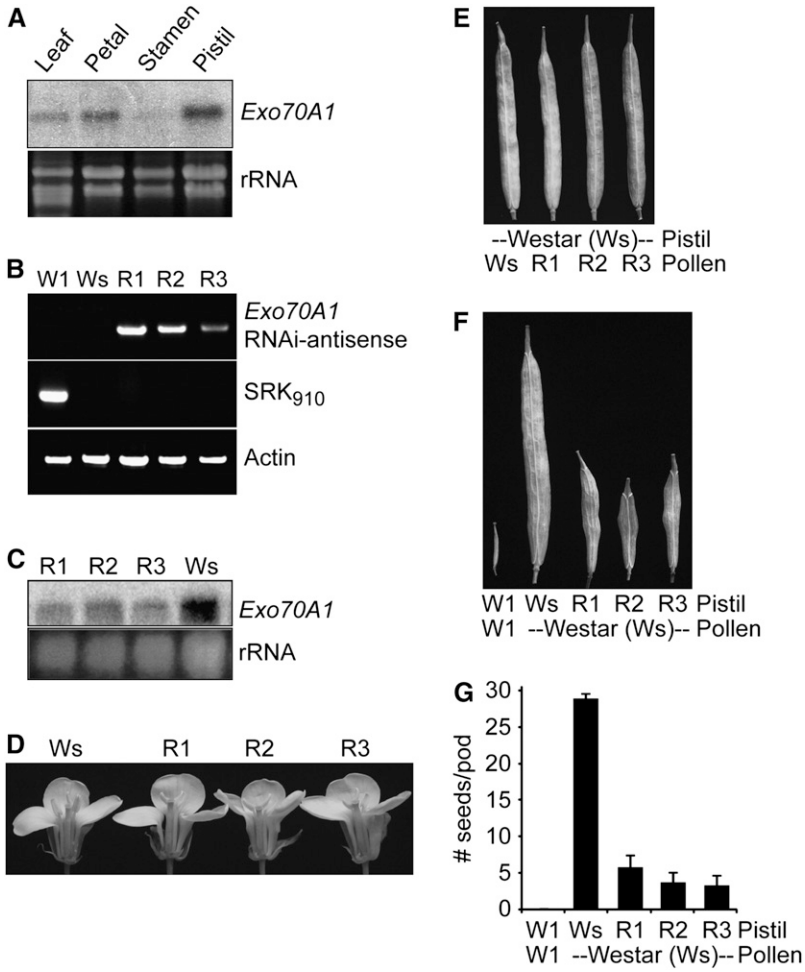

Figure 2. Reduced Expression Levels of *Exo70A1* in the Stigmas of Compatible *B. napus* Westar Causes Decreased Seed Production.

(A) *Exo70A1* RNA expression in different *B. napus* tissues. *Exo70A1* RNA is detected by RNA gel blot analysis in several tissues, with highest levels of expression in the pistil and lowest levels in the stamens. RNA was extracted from the W1 self-incompatible cultivar.

(B) DNA genotyping of the *Exo70A1* RNAi Westar lines. Three independent transgenic *B. napus* Westar lines, R1 to R3, carrying the $SLR1_{pro}$*Exo70A1* RNAi construct were generated. The presence of the *Exo70A1* RNAi construct in the R1-R3 lines was detected by PCR using sense and antisense primer combinations. Actin served as a positive control for the PCR reaction. The self-incompatible *B. napus* W1 line is identified by the presence of the S_{910} allele through the PCR detection of the SRK_{910} gene (Silva et al., 2001). The compatible *B. napus* Westar (Ws) line does not carry this self-incompatibility allele.

(C) *Exo70A1* expression in the stigmas of the *Exo70A1* RNAi Westar lines. All three independent transgenic *Exo70A1* RNAi Westar lines, R1 to R3, have reduced *Exo70A1* mRNA levels in the stigmas as shown by RNA gel blot analysis.

(D) The *Exo70A1* RNAi Westar lines produce flowers of wild-type appearance.

(E) The *Exo70A1* RNAi Westar lines produce wild-type pollen, which in turn produces full seedpods when used in pollinations with wild-type Westar pistils.

(F) and **(G)** The *Exo70A1* RNAi Westar stigmas, with reduced *Exo70A1* expression, have significantly reduced seed production in comparison to Westar stigmas when pollinated with compatible Westar pollen (*t* test, $P < 0.05$). Seedpods **(F)** and average number of seeds per pod **(G)** from the *Exo70A1* RNAi Westar (R1 to R3) plants. $n = 5$; error bars indicate ±SE.

decrease in Exo70A1 protein levels was observed after pollination (see Supplemental Figure 2 online). However, this would be difficult to detect, given the increased levels of *Exo70A1* in the S1 and S2 lines; in addition, this predicted effect would only occur in a small subset of the stigmatic cells, the stigmatic papillae in contact with pollen.

Exo70A1 Expression in the *Brassica* Stigma Is Necessary and Sufficient to Support Pollen Hydration, Germination, and Pollen Tube Penetration

With the establishment of the biological function of Exo70A1in *Brassica* stigmas, following pollination, we then investigated the cellular function of Exo70A1 in these responses. Pollen–stigma

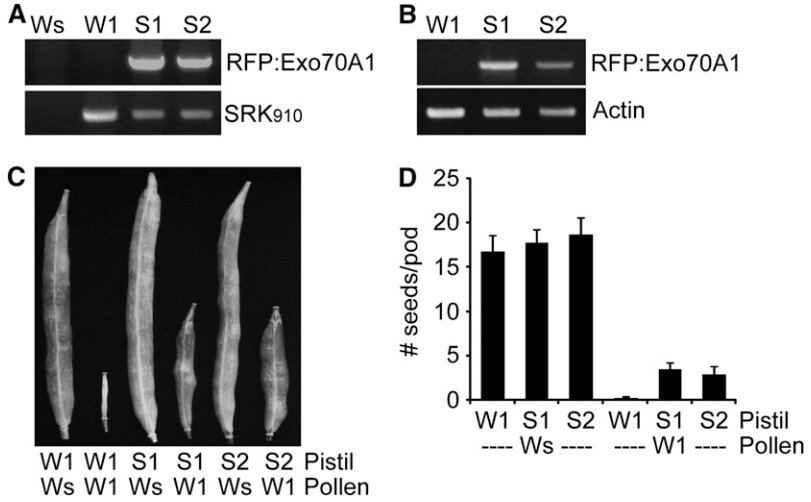

Figure 3. Expression of *RFP:Exo70A1* in the Stigmas of Self-Incompatible *B. napus* W1 Disrupts the Self-Incompatibility Response and Leads to Increased Seed Production.

(A) DNA genotyping of the *RFP:Exo70A1* W1 lines. Two independent transgenic *B. napus* W1 lines, S1 and S2, carrying the $SLR1_{pro}$*RFP:Exo70A1* (*B. napus Exo70A1*) construct were generated. The presence of *RFP:Exo70A1* in the S1 and S2 lines was detected using PCR with primer combinations specific to the $SLR1_{pro}$*RFP:Exo70A1* construct. The self-incompatible *B. napus* W1 line was identified by the presence of the S_{910} allele through the PCR detection of the SRK_{910} gene (Silva et al., 2001). The compatible *B. napus* Westar (Ws) line does not carry this self-incompatibility allele.
(B) *RFP:Exo70A1* expression in the stigmas of the *RFP:Exo70A1* W1 lines. The two independent transgenic W1 lines, S1 and S2, express *RFP:Exo70A1* in the stigmas, as shown by RT-PCR analysis (32 cycles; two biological replicates and three technical replicates).
(C) and **(D)** The *RFP:Exo70A1*-expressing W1 stigmas have significantly increased seed production in comparison to W1 stigmas when pollinated with self-incompatible W1 pollen (*t* test, $P < 0.05$). The *RFP:Exo70A1*-expressing W1 stigmas also produce full seedpods when pollinated with compatible Westar pollen, as expected. Seedpods **(C)** and average number of seeds per pod **(D)** from the *RFP:Exo70A1* W1 (S1 and S2) plants. $n = 5$; error bars indicate $\pm$SE.

interactions in the *Exo70A1* RNAi Westar lines and the *RFP:Exo70A1* W1 lines were observed more closely to examine pollen hydration and pollen tube penetration through the stigmatic surface (Figures 4 and 5). During control compatible *B. napus* Westar pollinations, the pollen grains rapidly hydrated within 4 min and continued to increase in diameter up to 10 min following pollination (Figures 4A to 4C). By contrast, in the control self-incompatible *B. napus* W1 pollinations, the pollen grains displayed very poor hydration due to the activated self-incompatibility pathway in the stigmatic papillae (Figures 4A, 4H, and 4I). Interestingly, Westar pollen on the *Exo70A1* RNAi Westar stigmas (R1 to R3) exhibited significantly reduced hydration (Figures 4A, 4F, and 4G). By contrast, W1 pollen on the *RFP:Exo70A1* W1 stigmas (S1 and S2) show significant increases in hydration (Figures 4A, 4D, and 4E). Thus, decreasing the levels of *Exo70A1* in Westar stigmas resulted in reduced pollen hydration in comparison to the Westar compatible control while increasing *Exo70A1* in W1 stigmas resulted in increased pollen hydration in comparison to the W1 self-incompatible control.

These results were also confirmed when aniline blue–stained, pollinated pistils were observed for pollen germination and pollen tube growth (Figure 5). At 2 h after pollination, control compatible *B. napus* Westar pistils had a large number of pollen grains adhered to the stigma, and these pollen grains had germinated and produced pollen tubes that penetrated the stigmatic surface (Figure 5B). By contrast, control self-incompatible *B. napus* W1 pistils did not have any pollen grains present (as expected) since the rejected pollen had failed to adhere and were washed away during the aniline blue staining (Figure 5A). Significantly, and in contrast with the control pollinations, the *Exo70A1* RNAi Westar stigmas had very few Westar pollen grains present (Figures 5C and 5D), and the *RFP:Exo70A1* W1 stigmas had a number of W1 pollen grains adhering to the stigmatic surface (Figures 5E, 5F, and 5M). Some of the pollen adhering to *RFP:Exo70A1* W1 stigmas had germinated to produce pollen tubes (Figures 5E and 5F). Thus, changes in Exo70A1 levels have a dramatic effect on pollen hydration and germination, affecting one of the earliest stages known to be blocked by the *Brassica* self-incompatibility response.

In addition to blocking pollen hydration, the *Brassica* self-incompatibility response can also block any pollen tubes, emerging from hydrated pollen grains, from penetrating the stigmatic surface. To investigate whether Exo70A1 has a role in this latter stage, pollen–stigma interactions in the *Exo70A1* RNAi Westar lines and the *RFP:Exo70A1* W1 lines were again examined at 8 h after pollination. While the W1 and Westar controls (Figures 5G and 5H) remain unchanged compared with 2 h after pollination (Figures 5A and 5B), Westar pollen on the *Exo70A1* RNAi Westar stigmas were eventually able to germinate (perhaps due to incomplete RNAi suppression) and produce pollen tubes (Figures 5I and 5J). However, the pollen tubes appeared quite

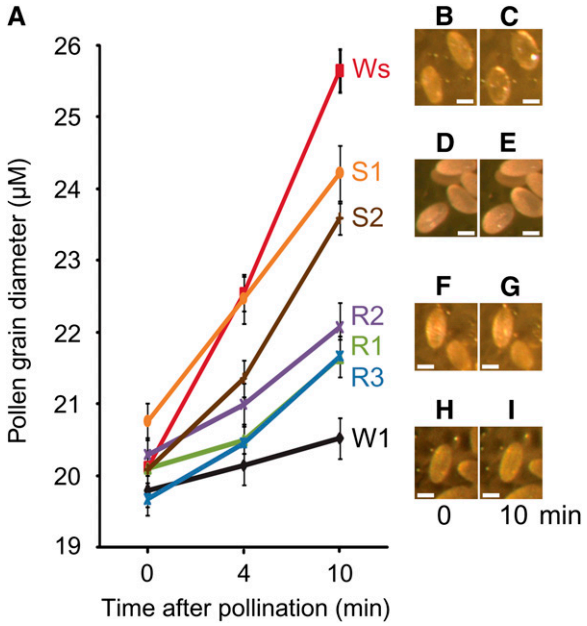

Figure 4. Altered Rates of Pollen Hydration on the *Exo70A1* RNAi Westar Stigmas and the *RFP:Exo70A1*-Expressing W1 Stigmas.

(A) Pollen hydration was detected by measuring the increasing pollen grain diameters (μM) measured at 0, 4, and 10 min after pollination. The *Exo70A1* RNAi Westar (R1 to R3) and control Westar (Ws) stigmas were pollinated with compatible Westar pollen. The *RFP:Exo70A1*-expressing W1 (S1 and S2) and control W1 stigmas were pollinated with self-incompatible W1 pollen. $n > 20$; error bars are ±SE.

(B) to **(I)** Representative images of hydrating pollen grains are shown at 0 and 10 min after pollination for a Westar stigma (**[B]** and **[C]**), an *RFP:Exo70A1*-expressing W1 stigma from the S2 line (**[D]** and **[E]**), an *Exo70A1* RNAi Westar stigma from the R2 line (**[F]** and **[G]**), and a W1 stigma (**[H]** and **[I]**). Bars = 20 μm.

stunted and were blocked from penetrating the stigmatic surface (Figures 5I and 5J). The *RFP:Exo70A1* W1 lines also had a number of self-incompatible W1 pollen that gave rise to stunted pollen tubes (Figures 5K and 5L). Thus, Exo70A1 is also required for successful pollen tube penetration through the stigmatic cell wall, and reducing *Exo70A1* levels in the stigma prevents the penetration of compatible Westar pollen tubes. Furthermore, the overexpression of *RFP:Exo70A1* was not able to completely break down this stage of the self-incompatibility response, although some pollen tubes successfully penetrated the stigmatic surface to produce seeds as shown in Figures 3C and 3D.

Exo70A1 Has a Conserved Function in the Stigmatic Papillae of *Arabidopsis*

Having established a critical role of *B. napus* Exo70A1 in *Brassica* pollen–stigma interactions, its role was also examined in *Arabidopsis*, a self-fertile species in the *Brassicaeae*. The putative ortholog for *B. napus Exo70A1* is *Arabidopsis Exo70A1* (see Supplemental Figures 1A and 1B online). Transgenic *Arabidopsis* lines carrying an *Arabidopsis* Exo70A1$_{pro}$GUS (for β-glucuronidase) construct displayed GUS expression in several tissues (see Supplemental Figure 3E online) and, interestingly, have strong GUS activity in the stigma of mature flowers (Figure 6A). This is a typical expression profile for genes that are active in the stigma during pollen–stigma interactions. Null mutants for *Arabidopsis Exo70A1* were previously shown to be slow-growing, semidwarf plants with an extended life span and defects in organ morphogenesis and fertility (Synek et al., 2006). To examine the pollen–stigma interactions in the *Arabidopsis exo70A1* mutants more closely, two independent T-DNA insertion lines as previously reported by Synek et al. (2006) were isolated (see Supplemental Figures 3A to 3D online). While Synek et al. (2006) reported that the *Arabidopsis exo70A1* mutant stigmas were immature in appearance at flower bud opening (stage 13; Smith et al., 1990), we found that this was variable and that elongated stigmatic papillae could be observed (Figure 6G; see Supplemental Figures 3D, 4D, and 4E online). When individual wild-type *Arabidopsis* pollen grains were placed on wild-type stigmatic papillae, 91% of the pollen grains were fully hydrated, as shown in Figure 6B. Conversely, elongated stigmatic papillae from the *exo70A1* mutant lines failed to support wild-type pollen hydration. Only 45% of the wild-type pollen placed on the *exo70A1* stigmatic papillae showed any hydration, with these pollen grains being only partially hydrated (Figure 6C).

To confirm that the loss of pollen hydration was correlated with the loss of Exo70A1, heterozygous *exo70A1-1 Arabidopsis* plants were transformed with the SLR1$_{pro}$*RFP:Exo70A1* (*B. napus Exo70A1*) construct, and two independent lines (S4 and S14) of homozygous *exo70A1-1* mutants expressing *RFP:Exo70A1* in the stigma were recovered (Figures 6D and 6E). Detailed pollination studies were then performed on stigmas from Columbia-0 (Col-0), the *exo70A1* mutant, and the S4 and S14 plants transformed with the *RFP:Exo70A1* construct with aniline blue staining, which is used to detect pollen tubes. As expected for the self-fertile Col-0 control, the stigmas were covered with adhered pollen grains and numerous pollen tubes could be detected (Figures 6F and 6I; see Supplemental Figure 4C online). By contrast, when wild-type Col-0 pollen were used to pollinate the *Arabidopsis exo70A1* mutant stigmas, the pollen were largely rejected with very few pollen grains detected following aniline blue staining (Figures 6G and 6I; see Supplemental Figures 4D and 4E online). While the *exo70A1* mutant showed variability in papillar elongation, there was no adherance of compatible pollen, regardless of whether papillae were short or elongated (Figures 6G; see Supplemental Figures 4D and 4E online). The expression of the RFP:Exo70A1 fusion protein in the *exo70A1-1* mutant stigmas fully restored the ability of compatible wild-type Col-0 pollen to adhere to the *exo70A1* stigmas and produce pollen tubes (S14/*exo70A1-1*; Figures 6H and 6I; see Supplemental Figures 4G and 4H online). Both the control Col-0 and the rescued S14/*exo70A1-1* pollinated pistils produced large numbers of seeds per silique, while no seeds were detected in the *exo70A1* siliques pollinated with Col-0 pollen (Figures 6J and 6K). Thus, the *Brassica* and *Arabidopsis* Exo70A1 share conserved functions in the stigma, namely, promoting pollen hydration and pollen tube growth of compatible pollen, and loss of Exo70A1 produces a phenotype that is correlated with the *Brassica* self-incompatibility response.

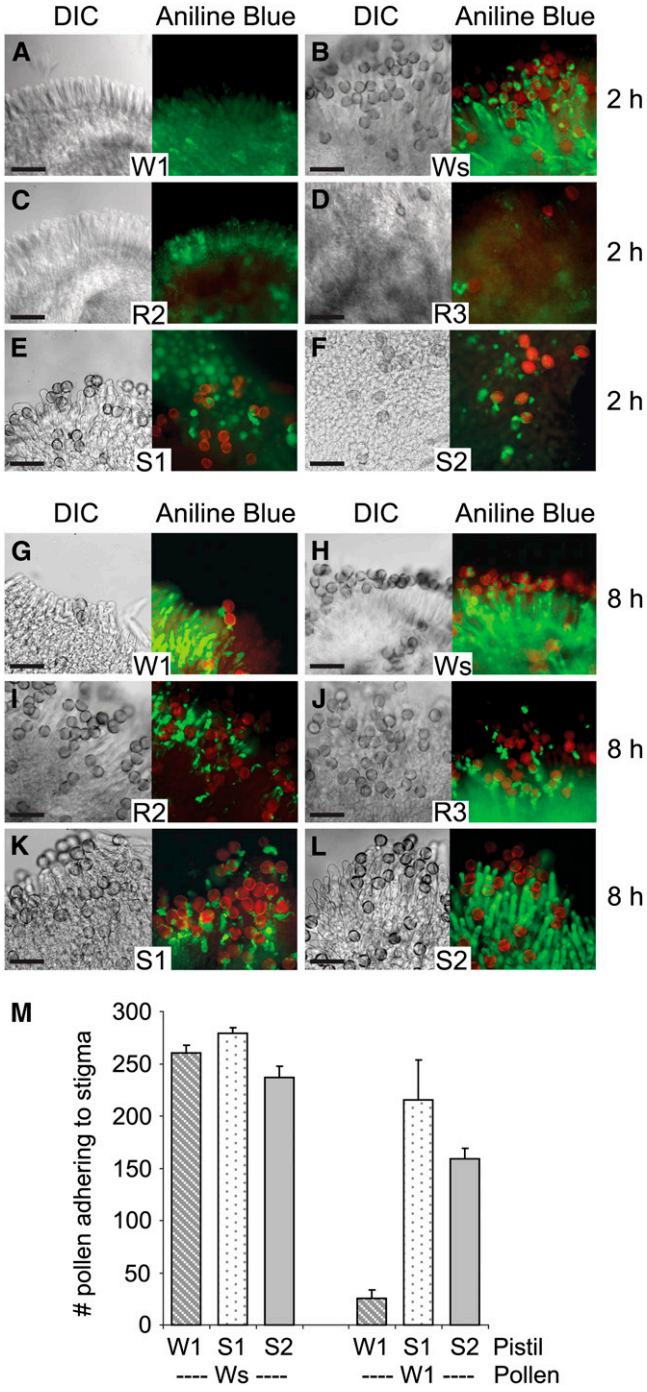

Figure 5. Altered Pollen Germination and Pollen Tube Growth on the *Exo70A1* RNAi Westar Stigmas and the *RFP:Exo70A1*-Expressing W1 Stigmas.

(A) to **(L)** Pollen attachment and pollen tube growth at 2 h (**[A]** to **[F]**) and 8 h (**[G]** to **[L]**) following pollination. The *Exo70A1* RNAi Westar R2 and R3 stigmas (**[C]**, **[D]**, **[I]**, and **[J]**) and control Westar (Ws) stigmas (**[B]** and **[H]**) were pollinated with compatible Westar pollen. The *RFP:Exo70A1* W1 S1 and S2 stigmas (**[E]**, **[F]**, **[K]**, and **[L]**) and control W1 stigmas (**[A]** and **[G]**) were pollinated with self-incompatible W1 pollen. Differential interference contrast (DIC) images and images of aniline blue–stained pistils are shown. The aniline blue fluorescence from the stigma and pollen tubes are shown in green and overlaid with the red autofluorescence from pollen grains. The *Exo70A1* RNAi Westar stigmas support a reduced attachment of Westar pollen grains as well as reduced pollen tube growth (**[C]**, **[D]**, **[I]**, and **[J]**). The *RFP:Exo70A1*-expressing W1 stigmas support increased attachment of self-incompatible W1 pollen as well as increased pollen tube growth (**[E]**, **[F]**, **[K]**, and **[L]**). Bars = 100 μm.

(M) Average number of self-incompatible W1 and compatible Westar pollen grains attached to the *RFP:Exo70A1*-expressing W1 stigmas. The number of pollen grains present on the *RFP:Exo70A1*-expressing W1 stigmas (S1 and S2) was counted 8 h following either a Westar or W1 pollination. The expression of *RFP:Exo70A1* causes a significant increase in the number of self-incompatible W1 pollen grains attaching to the S1 and S2 stigmas in relation to W1 stigmas (*t* test, $P < 0.05$; $n = 4$).

Exo70A1 Is Localized to the Plasma Membrane of Mature Stigmatic Papillae and Disappears from the Plasma Membrane Following Compatible Pollinations

Having established that RFP:Exo70A1 (*B. napus Exo70A1*) can rescue the stigmatic defect in the *Arabidopsis exo70A1* mutants, we then examined where the RFP:Exo70A1 is localized in the stigma during pollinations. As the *Arabidopsis* stigmatic papillae are smaller and less dense than those of *Brassica*, the RFP fluorescence from the elongated papillae could readily be visualized in these lines using confocal microscopy. Segregating progeny from heterozygous *exo70A1-1 Arabidopsis* plants transformed with the *RFP:Exo70A1* construct were genotyped to identify both the wild type (S14/Col-0) and homozygous mutant (S14/*exo70A1-1*) (Figure 7). Confocal imaging of unpollinated S14/Col-0 stigmas revealed RFP fluorescence localized to the plasma membrane of stigmatic papillae from freshly opened flowers (stage 13; Figures 7A and 7B). Interestingly, the plasma membrane localization of RFP:Exo70A1 is only achieved at maturity as an examination of stigmas from unopened flower buds (stage 12) revealed RFP fluorescence localized to internal punctate structures, a staining pattern reminiscent of Golgi (Figure 7C) (Boevink et al., 1998). In other systems, Exo70 functions as a spatial landmark at the plasma membrane for the assembly of the exocyst complex, which in turn tethers secretory vesicles for exocytosis (Boyd et al., 2004). Thus, the plasma membrane localization of RFP:Exo70A1 in mature stigmatic papillae is consistent with Exo70 functioning as a spatial landmark. The localization of RFP:Exo70A1 was also examined in S14/*exo70A1-1*, and RFP:Exo70A1 was found to localize to the plasma membrane, though to a lesser extent than for S14/Col-0 with some internal punctate structures remaining (Figure 7D). Since the SLR1 promoter was used to drive the expression of *RFP:Exo70A1* in the *exo70A1* homozygous mutants, only the stigmatic fertility defect is fully restored in these plants (Figure 6). The overall growth defect remains in these plants (Synek et al., 2006) (see Supplemental Figure 3C online) and may be related to some of the RFP:Exo70A1 remaining within the cells.

The plasma membrane localization of RFP:Exo70A1 was verified by crossing the S14/Col-0 line to a green fluorescent protein (GFP):δ-TIP vacuolar marker line, since the vacuolar membrane can often be in close proximity to the plasma

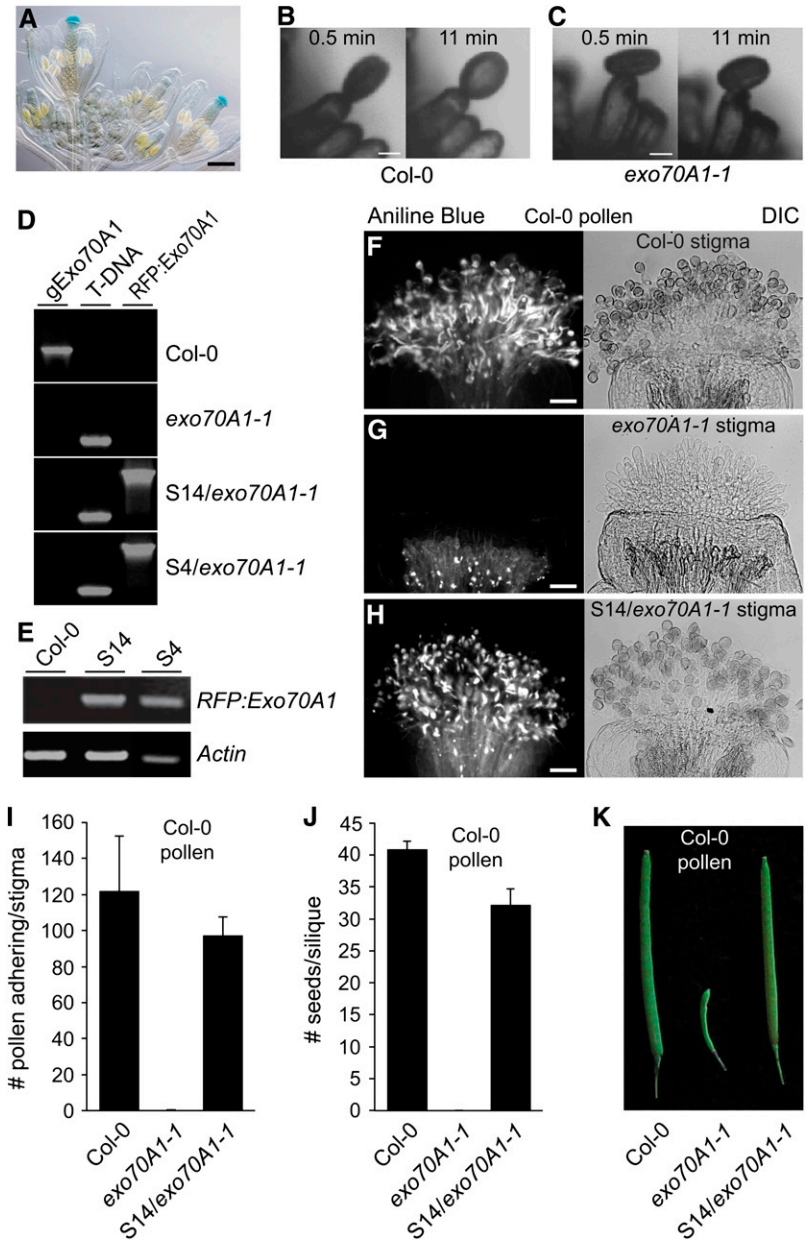

Figure 6. The *Arabidopsis Exo70A1* Gene Shares a Conserved Function with *B. napus Exo70A1* in the Stigma during Pollen–Stigma Interactions.

(A) *Arabidopsis* Exo70A1$_{pro}$GUS shows strong GUS expression in stigmatic tissues. Bar = 250 μm.

(B) and **(C)** Pollen hydration on an *Arabidopsis* Col-0 or *exo70A1* stigmatic papilla. Pollen hydration was observed following the placement of a single wild-type Col-0 pollen grain on top of either a wild-type Col-0 **(B)** or *exo70A1-1* **(C)** stigmatic papilla using a micromanipulator. Images are shown at 0.5 and 11 min after pollination. Pollen grain hydration is impaired on the *exo70A1-1* mutant stigma, while full hydration is observed for the wild-type compatible Col-0 stigma. Bars = 10 μm.

(D) DNA genotyping of the *RFP:Exo70A1*-expressing *Arabidopsis* lines. Two independent transgenic *Arabidopsis* lines, S4 and S14, carrying the SLR1$_{pro}$*RFP:Exo70A1* construct were generated. This construct was introduced into a heterozygous Exo70A1/*exo70A1-1 Arabidopsis* plant (see Supplemental Figures 3A to 3D online), and transformed heterozygous plants were recovered. The next generation was then screened for segregating wild-type Col-0 and homozygous *exo70A1-1* plants carrying the *RFP:Exo70A1* construct. The presence of *RFP:Exo70A1* in the S4 and S14 lines was detected by PCR using sense and antisense primer combinations. The *exo70A1-1 Arabidopsis* plants were identified by the presence of T-DNA (see Supplemental Figures 3A and 3B online). The undisrupted Exo70A1 gene (gExo70A1) was detected using gene-specific primers.

(E) *RFP:Exo70A1* expression in the pistils of the *RFP:Exo70A1 Arabidopsis* lines. The two independent transgenic *Arabidopsis* lines, S4 and S14, express *RFP:Exo70A1* in the pistils, as shown by RT-PCR analysis (28 cycles; two biological replicates and four technical replicates).

(F) to **(H)** Pollen attachment and pollen tube growth in *Arabidopsis* pistils from a wild-type Col-0 **(F)**, *exo70A1-1* mutant **(G)**, and the *exo70A1-1* mutant

membrane in stigmatic papillae (Figure 7E; see Supplemental Figure 5A online). The green fluorescence from the GFP:δ-TIP marker outlines the membranes of the central vacuole as well as the apical vacuolar network (previously described in Iwano et al., 2007). Figure 7E shows a tip of a stigmatic papilla where the GFP fluorescence from the vacuolar membranes are distinct from the plasma membrane–localized RFP:Exo70A1. Furthermore, the S14/Col-0 line was crossed to a ST:GFP Golgi marker line to examine the Golgi-like RFP:Exo70A1 punctate structures in immature stigmatic papillae, and colocalization was observed, indicating that these structures are Golgi (Figure 7F; see Supplemental Figures 5C to 5E online). Finally, the RFP:Exo70A1 localization pattern was examined following compatible pollinations in the wild-type S14/Col-0 stigmatic papillae. After several minutes, we consistently observed that the RFP fluorescence disappeared from the plasma membrane in stigmatic papillae that were in contact with Col-0 pollen. Examples of this are shown in Figures 7G and 7H, where at 8 and 10 min after pollination, the RFP:Exo70A1 cannot be detected in the plasma membrane of stigmatic papillae that are in contact with the pollen grains, while the neighboring unpollinated stigmatic papillae appear to be unchanged. Thus, there are substantial changes in the subcellular distribution of RFP:Exo70A1 following a compatible pollination.

Activation of SRK and ARC1 Results in the Proteasomal Localization of Exo70A1 in Tobacco BY-2 Cells

Given the critical role of Exo70A1 in the stigmatic papillae in the early stages following compatible pollinations, Exo70A1 would be an effective target for the self-incompatibility pathway to promote pollen rejection. Given ARC1's activity as an E3 ligase, its ability to bind and ubiquitinate Exo70A1, and the fact that ARC1 localizes to the proteasome in BY-2 suspension cells in the presence of active SRK (Stone et al., 2003), we tested whether ARC1 could target *Brassica* Exo70A1 to the proteasome. Constructs generated with different epitope tags at the N terminus of each protein (Figure 8A) were transiently expressed in BY-2 cells and followed by fluorescence microscopy to determine subcellular localization patterns. Both GFP:ARC1 and RFP:Exo70A1, as well as the RFP control, were predominantly distributed throughout the cytosol when expressed either alone or together (Figures 8B to 8K). When a constitutively active SRK kinase domain was added as a GST:kinase fusion, there was no effect on the RFP control (Figures 8L and 8M), but a redistribution of both ARC1 and Exo70A1 to punctate structures generally around the perinuclear region was observed (Figures 8N to 8R). A similar pattern was also seen when *Arabidopsis* Exo70A1 was coexpressed with ARC1 and GST:SRK (Figures 8S to 8W). The proteasomal subunit, RPT2A, was found to colocalize to these punctate structures with Exo70A1 (Figures 9A to 9D), and this pattern overlapped with the Concanavalin A marker for the endoplasmic reticulum (Figures 9E to 9H). Two endosomal markers were also tested; Syp21, a marker for the late endosome/prevacuolar compartment, and Syp42, which resides in the trans-Golgi network (Sanderfoot et al., 2001; Samaj et al., 2005). While Syp42 did not colocalize with the Exo70A1/ARC1 subcellular structures (Figure 9P), there was some overlap with the Syp21 marker (Figure 9H). Thus, these results suggest that SRK triggers the relocalization of both ARC1 and Exo70A1 to endoplasmic reticulum–associated proteasomes and that there may be some association between the ARC1 and Exo70A1 proteins with the late endosome/prevacuolar compartment.

DISCUSSION

In the *Brassicaceae*, a complex pollen recognition system is present in the stigma to ensure that stigmatic resources are only provided to compatible pollen grains. In addition, the self-incompatibility response is superimposed on this pathway to prevent self pollen from being accepted, and this has been proposed to occur by disrupting compatible pollen–stigma interactions (Dickinson, 1995). While many players in the *Brassica* self-incompatibility response have been identified (Takayama and Isogai, 2005), the molecules and mechanism underlying this response and its ability to interrupt compatibility signaling has remained unresolved thus far. We previously showed that the ARC1 E3 ligase functions as a downstream substrate for SRK and suppression of ARC1 in self-incompatible W1 lines led to partial breakdown of self-incompatibility (Gu et al., 1998; Stone et al., 1999, 2003). In this study, we have identified Exo70A1 as an interactor and substrate for ARC1.

Figure 6. (continued).

expressing *RFP:Exo70A1* (S14/*exo70A1-1*) **(H)**. All pistils were pollinated with compatible *Arabidopsis* Col-0 pollen and then stained with aniline blue to visualize the pollen attachment and pollen tube growth. As expected, abundant pollen tube growth is observed on the compatible wild-type Col-0 stigma. The *exo70A1-1* mutant stigma does not support any pollen attachment or pollen tube growth, and only background fluorescence is observed in the aniline blue–stained stigma. The expression of *RFP:Exo70A1* in the *exo70A1-1* stigma rescues this defect and restores pollen attachment and pollen tube growth. Bars = 50 μm.

(I) Average number of attached compatible Col-0 pollen grains on stigmas from wild-type Col-0, the *exo70A1-1* mutant, or the *exo70A1-1* mutant expressing *RFP:Exo70A1* (S14/*exo70A1-1*) ($n = 5$; error bars indicate ±SE). The number of adhered pollen for the *exo70A1-1* mutant is significantly lower than for either Col-0 or S14/*exo70A1-1* (*t* test, $P < 0.05$), while the results for the rescued S14/*exo70A1-1* stigmas are not significantly different from those for Col-0 (*t* test, $P > 0.05$).

(J) and **(K)** Average number of seeds per silique (**[J]**; $n = 7$) and siliques **(K)** from Col-0, *exo70A1-1*, and the *exo70A1-1* mutant expressing *RFP:Exo70A1* (S14/*exo70A1-1*) pistils following a Col-0 pollination. Following a compatible Col-0 pollination, no seeds are produced from *exo70A1-1* mutant pistils, while the expression of *RFP:Exo70A1* in the *exo70A1-1* mutant stigma restores full seed production. Seed set values for Col-0, the *exo70A1-1* mutant, and S14/*exo70A1-1* are all significantly different from each other (*t* test, $P < 0.05$).

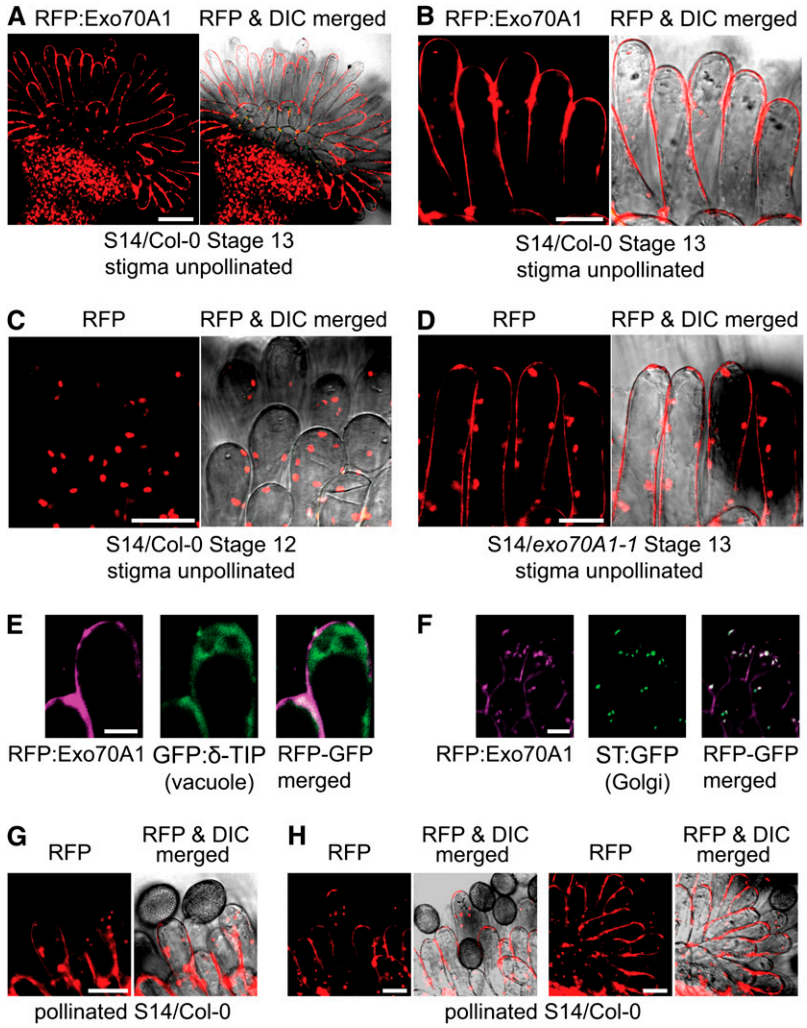

Figure 7. Characterization of *RFP:Exo70A1* Lines in Col-0 and the *exo70A1-1* Mutant Background.

RFP and RFP/DIC merged images of stigmas from different stages are marked.
(A) and **(B)** In mature stigmas (stage 13) from the S14/Col-0 line, RFP:Exo70A1 is found at the plasma membrane.
(C) In immature stigmas (stage 12) from the S14/Col-0 line, RFP:Exo70A1 is localized to internal structures that are reminiscent of Golgi.
(D) In the S14/*exo70A1-1* mature stigmas, RFP:Exo70A1 is localized to the plasma membrane, but some also remains inside the cells.
(E) A stage 13 Col-0 stigmatic papilla expressing both RFP:Exo70A1 and a GFP:δ-TIP vacuolar marker. The GFP:δ-TIP marker outlines the membranes of the central vacuole as well as the vacuolar network in the apical region. The localization of the GFP:δ-TIP marker is distinct from that of RFP:Exo70A1, which confirms the plasma membrane localization of RFP:Exo70A1.
(F) Stage 12 Col-0 stigmatic papillae expressing both RFP:Exo70A1 and a ST:GFP Golgi marker. The ST:GFP Golgi marker overlaps with RFP:Exo70A1, confirming the Golgi localization of RFP:Exo70A1 in immature stigmatic papillae.
(G) and **(H)** Following a Col-0 pollination, RFP:Exo70A1 disappears from the plasma membrane in the S14/Col-0 lines.
(G) A pollinated stigma at 8 min after pollination.
(H) A different pollinated stigma at 10 min after pollination. The RFP image on the left and the corresponding merged image show an area with several attached pollen grains, while the right RFP image and the corresponding merged image show an area with a single attached pollen grain. Note the absence of RFP fluorescence at the plasma membrane in papillae that are in contact with a pollen grain.
Bars = 50 μm in **(A)**, 20 μm in **(B)** to **(D)**, **(G)**, and **(H)**, and 10 μm in **(E)** and **(F)**.

Exo70 is a subunit of the exocyst complex, which functions in regulated or targeted vesicle trafficking to the plasma membrane in yeast and animal systems (Munson and Novick, 2006; He and Guo, 2009). Various processes regulated by the exocyst include polarized exocytosis during yeast budding, neurite outgrowth, insulin-stimulated trafficking of the GLUT4 transporter to the plasma membrane in adipocyte cells, and selective tethering of vesicles to the apical or basolateral membranes in polarized epithelial cells (Lipschutz and Mostov, 2002; EauClaire and Guo, 2003; Folsch et al., 2003; Inoue et al., 2003; Oztan et al., 2007).

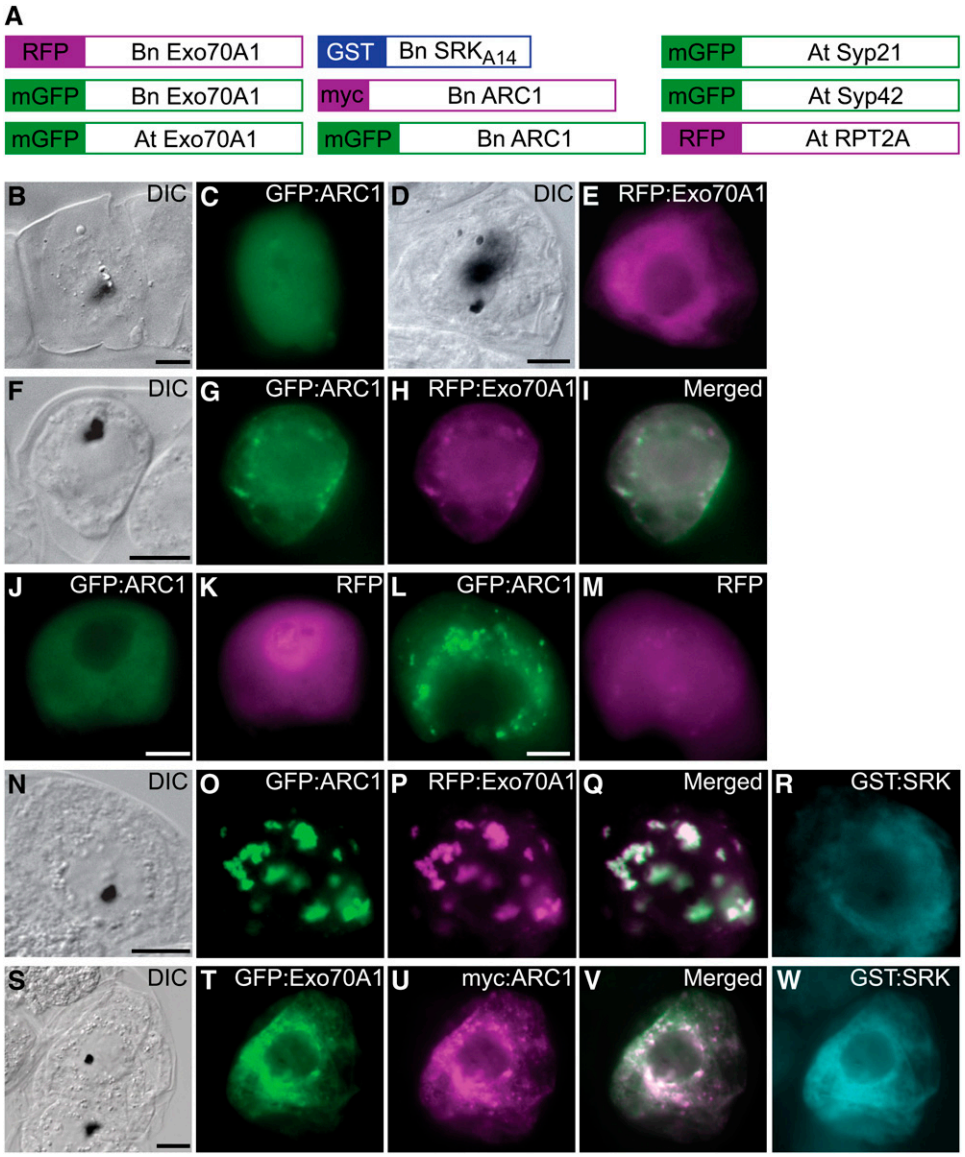

Figure 8. The Effect of SRK and ARC1 on the Subcellular Localization of Exo70A1 in BY-2 Cells.

(A) Schematics of different constructs used to transiently transform tobacco BY-2 cells using particle bombardment. Full-length coding regions were fused to different tags, except for SRK_{A14}, where the cytosolic kinase domain was fused to GST as described by Stone et al. (2003). Bn, *Brassica napus*; At, *Arabidopsis thaliana*.

(B) to **(E)** Single transformations with either GFP:ARC1 (**[B]** and **[C]**) or RFP:Exo70A1 (*B. napus* Exo70A1) (**[D]** and **[E]**). Cytosolic localization is observed for both fusion proteins.

(F) to **(I)** Double transformation and coexpression of GFP:ARC1 and RFP:Exo70A1 (*B. napus* Exo70A1). Cytosolic localization is observed for both proteins.

(J) and **(K)** Control double transformation and coexpression of GFP:ARC1 and RFP alone.

(L) and **(M)** Control triple transformation and coexpression of GST:SRK (kinase domain only), GFP:ARC1, and RFP alone. The coexpression of the active GST:SRK causes ARC1 to localize to punctate perinuclear structures as previously published (Stone et al., 2003; Samuel et al., 2008) but has no effect on RFP. GST:SRK remains cytosolic, as previously published (Stone et al., 2003; Samuel et al., 2008).

(N) to **(R)** Triple transformation and coexpression of GST:SRK (kinase domain only), GFP:ARC1, and RFP:Exo70A1 (*B. napus* Exo70A1). Subcellular localization of Exo70A1 and ARC1 to the perinuclear region is observed. GST:SRK remains cytosolic.

(S) to **(W)** Triple transformation and coexpression of GST:SRK (kinase domain only), GFP:ARC1, and RFP:Exo70A1 (*Arabidopsis* Exo70A1). Subcellular localization of *Arabidopsis* Exo70A1 and ARC1 to the perinuclear region is also observed.

Black dots in the DIC images are the tungsten particles used for the bombardments. Areas of white in the merged images indicate overlapping localization patterns. Bars = 10 μm.

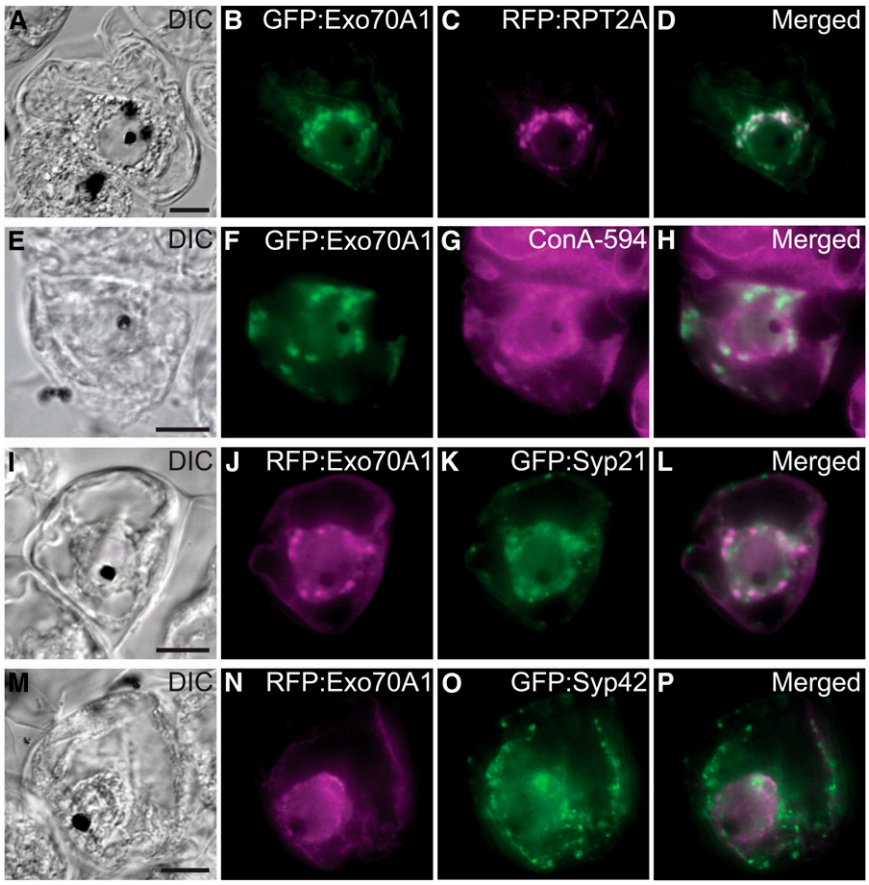

Figure 9. The Subcellular Localization of *B. napus* Exo70A1 in BY-2 Cells in Relation to Different Marker Proteins.

(A) to **(D)** Quadruple transformation and coexpression of RFP:RPT2A with GFP:Exo70A1, myc:ARC1, and GST:SRK. Exo70A1 colocalizes with the proteasomal subunit, RPT2A.

(E) to **(H)** Triple transformations and coexpression of GST:SRK, myc:ARC1, and GFP:Exo70A1, followed by ConA-594 staining. Concanavalin A stains the endoplasmic reticulum and overlaps with the Exo70A1/ARC1 subcellular structures.

(I) to **(P)** Quadruple transformations and coexpression of GST:SRK, myc:ARC1, RFP:Exo70A1, and either GFP:Syp21 (**[I]** to **[L]**) or GFP:Syp42 (**[M]** to **[P]**). Syp21 is a marker for the late endosome/prevacuolar compartment, and Syp42 was shown to reside in the trans-Golgi network (Sanderfoot et al., 2001; Samaj et al., 2005). There is a bit of overlap of the Exo70A1/ARC1 subcellular structures with Syp21.

GST:SRK remains cytosolic, and myc:ARC1 colocalizes with Exo70A1 to the punctate structures as shown in Figures 8N to 8R and previously published (Stone et al., 2003). Black dots in the DIC images are the tungsten particles used for the bombardments. Areas of white in the merged images indicate overlapping localization patterns. Bars = 10 μm.

The exocyst complex consists of eight individual subunits: Sec3, Sec5, Sec6, Sec8, Sec10, Sec15, Exo70, and Exo84 (Guo et al., 1999; Matern et al., 2001). In plants, the role of the exocyst is not as well established, though plant genomes are known to contain genes predicted to encode all eight exocyst subunits, and evidence is accumulating that the plant exocyst complex has similar functions to those seen in yeast and animal systems (Zárský et al., 2009). Interestingly, in contrast with mammalian and yeast counterparts, the majority of the predicted plant exocyst subunits exist as multiple copies with only a few of these genes having assigned functions (Synek et al., 2006; Hala et al., 2008; Chong et al., 2009).

Several *Arabidopsis* exocyst subunit genes, *Sec5*, *Sec6*, *Sec8*, *Sec15a*, and *Exo70A1*, have been found to play a role in polarized pollen tube growth (Cole et al., 2005; Hala et al., 2008), root hair elongation (Wen et al., 2005), and polar growth and development (Synek et al., 2006). Synergistic interactions between various exocyst subunits have also been observed when mutant combination of the various exocyst subunits enhanced the severity of the short hypocotyl phenotype seen in the *exo70A1* single mutants (Synek et al., 2006; Hala et al., 2008). Also, recent evidence demonstrated the assembly of the *Arabidopsis* exocyst subunits as a complex, and the increased localization of Sec6, Sec8, and Exo70A1 at the tip of the growing pollen tube (Hala et al., 2008). We have now uncovered a role for Exo70A1 in the stigma in response to compatible pollen, in addition to the other biological roles previously identified in experiments using the *exo70A1* mutant (Synek et al., 2006).

Through a functional analysis of *Exo70A1* in both compatible and incompatible *B. napus* lines, as well as compatible *Arabidopsis*, we have unraveled a number of aspects of Exo70A1 function during pollen–stigma interactions. First, Exo70A1 was found to be a novel factor required in the stigma for compatible pollinations. The suppression of Exo70A1 expression in the stigma was correlated with a loss of compatible pollen recognition and, furthermore, mimicked the self-incompatibility rejection response (reduced pollen hydration and pollen tube growth). Also, this defect in the stigmas of *Arabidopsis exo70A1* null mutants can be rescued by the stigma-specific expression of *Exo70A1*. This role was found in both *Brassica* and *Arabidopsis*, which diverged over 20 million years ago (Schranz et al., 2007) and thus suggests an evolutionarily conserved function for Exo70A1 in the dry stigmas of the *Brassicaceae*. Second, our work revealed a mechanism by which the self-incompatibility response targets compatibility factors to cause pollen rejection (likely via ARC1-mediated ubiquitination of Exo70A1). An increased level of *B. napus* Exo70A1 in the stigmas of self-incompatible W1 plants was able to partially overcome self-incompatibility, indicating that this pathway negatively regulates Exo70A1.

In the *Brassicaceae*, genetic screens have been largely unsuccessful in identifying stigmatic factors that are required at the early stages of compatible pollen recognition and acceptance (Edlund et al., 2004). This may be explained by these compatibility factors in the stigma having a more ubiquitous expression and role, such as that seen for Exo70A1 (Synek et al., 2006). Interestingly and in contrast with this, the genes encoding self-incompatibility factors, such as *SRK* and *ARC1*, have evolved a stigma-specific pattern of expression (Gu et al., 1998; Takasaki et al., 2000). The requirement of Exo70A1 for early stigmatic responses to compatible pollen points to the potential involvement of polarized secretion for delivering stigmatic resources to the site of pollen attachment (for pollen hydration and pollen tube penetration through the stigmatic cell wall). We propose that this occurs through the activation of the exocyst's function at the plasma membrane for vesicle tethering and fusion. It is interesting that we only observed Exo70A1 localization to the plasma membrane of stigmatic papillae in fully developed flowers and is consistent with a stigmatic papillar function of responding to pollen upon flower opening. The presence of Exo70A1 along the entire papillar plasma membrane suggests that another regulatory event occurs at the pollen contact site to promote localized exocyst assembly and vesicle docking. This is supported by the observed disappearance of Exo70A1 from the plasma membrane following pollen contact. In yeast, Sec3p and Exo70 mark the sites on the plasma membrane where exocyst assembly will occur through actin-dependent trafficking of six other exocyst subunits to mediate vesicle tethering (Boyd et al., 2004). For the insulin-stimulated glucose uptake in adipocyte cells, there is also a highly regulated process of exocyst complex tethering of preloaded GLUT4 glucose transporter-containing vesicles to the plasma membrane (Inoue et al., 2003). Insulin perception results in the activation of the TC10 G-protein, which in turn leads to the relocalization of Exo70 to lipid raft domains in the plasma membrane. The exocyst complex is then assembled and tethers GLUT4 vesicles to the plasma membrane (Inoue et al., 2003, 2006).

The proposed role for Exo70A1 in the polarized secretion of stigmatic papillar resources to the compatible pollen grain is highly consistent with the dry stigma system, and a reasonable model would be the delivery of vesicles containing aquaporins for increased water permeability (to allow pollen hydration), as well as cell wall–modifying enzymes (to allow pollen tube penetration through the stigma). In the self-incompatibility response, the inhibition of Exo70A1 would prevent these putative vesicles from fusing with the plasma membrane and result in the rapid and effective rejection of self pollen. However, the question does arise as to whether vesicular transport to the pollen attachment site occurs in the stigmatic papilla. In *Brassica*, previous studies have discovered that, following the treatment of the stigma with a compatible pollen coat extract, there is an accumulation of vesicle-like structures and a rapid expansion of the outer cell wall layer in the stigmatic papillae (Elleman and Dickinson, 1990, 1996). The vesicle-like structures accumulated in the apoplast, and this response was independent of de novo protein synthesis (Elleman and Dickinson, 1990, 1996). This suggests a posttranslational cellular event, consistent with the idea of preloaded vesicles being targeted for secretion. Also, the rapid expansion of the outer cell wall layer may be due to released enzymes modifying the cell wall for pollen tube growth through the papillar cell wall. Interestingly, in renal-collecting duct cells, components of the exocyst have been associated with intracellular vesicles carrying aquaporins, which are thought to fuse with the plasma membrane to increase water permeability (Barile et al., 2005).

A more recent observation has been the vacuolar movement in the stigmatic papilla in response to compatible pollen (Iwano et al., 2007). The vacuolar network was found to orient itself toward the compatible pollen attachment site, and the vacuolar changes were dependent upon an establishment of filamentous actin bundles in the stigmatic papilla, in close proximity to the pollen attachment site (Iwano et al., 2007). By contrast, self-incompatible pollinations were associated with a decrease in actin bundles and disruption of the vacuolar network in the stigmatic papilla (Iwano et al., 2007). Whether Exo70 and the exocyst complex are directly participating in the movement of the vacuolar network remains to be determined. In summary, we have identified Exo70A1 as a key protein at the interface of the pollen compatibility and self-incompatibility response pathways in the stigma.

METHODS

Yeast Two-Hybrid Screen, in Vitro Binding, and Ubiquitination Assays

To identify potential substrates regulated by ARC1, different domains of ARC1 were used to screen a pistil cDNA yeast two-hybrid library as previously described (Gu et al., 1998), and a single positive interaction was isolated with the ARC1 N-terminal domain (which is thought to serve as a potential substrate binding domain; Stone et al., 2003). Using BLAST searches at the National Center for Biotechnology Information and The Arabidopsis Information Resource, the *Brassica napus* cDNA was predicted to encode a protein with sequence similarity to Exo70s and was named *Exo70A1* due to its highest sequence similarity to *Arabidopsis thaliana Exo70A1* (see Supplemental Figures 1A and 1B online). The amino acid sequence alignment of *B. napus* Exo70A1 to *Arabidopsis* Exo70A1 was generated from the BLAST searches and edited manually.

For in vitro binding studies, His6:Exo70A1:FLAG (*B. napus* Exo70A1) and GST:ARC1 fusion proteins were expressed in *Escherichia coli* BL21 (DE3)pLysS cells and purified using Ni-NTA agarose beads (Novagen) or GSH agarose beads (Sigma-Aldrich), respectively, as previously described (Gu et al., 1998). Binding assays were set up using 0.5 μg of His6:Exo70A1:FLAG and 0.3 μg of either GST or GST:ARC1 as previously described. Protein gel blot analyses were performed using rabbit anti-ARC1, mouse anti-His (Novagen), mouse anti-FLAG (Sigma-Aldrich), or rabbit anti-GST (Santa Cruz) primary antibodies and anti-rabbit or anti-mouse secondary antibodies (KPL), followed by detection with the Enhanced Chemiluminescence Detection Kit (GE Amersham).

Ubiquitination of purified His6:Exo70A1:FLAG protein by GST:ARC1 was performed as previously described (Stone et al., 2003) using the *Arabidopsis* E2 enzyme, UBC7, and the yeast E1 enzyme. The ubiquitination assays were fractionated on a 7% SDS-PAGE gel followed by protein gel blot analysis using anti-FLAG antibodies (Sigma-Aldrich).

B. napus Westar and W1 Transgenic Lines

B. napus transgenic lines were created as previously described (Stone et al., 1999). For the *Exo70A1* RNAi Westar lines, PCR was used to tailor a double-stranded RNAi construct (Samuel and Ellis, 2002), using the N-terminal 678 nucleotides of the *B. napus Exo70A1* open reading frame, behind the strong stigma-specific SLR1 promoter (Franklin et al., 1996; Fobis-Loisy et al., 2007). The binary vector p1665 containing the SLR1 promoter was digested with *Sma*I and *Bam*HI to ligate the RNAi construct (for primers, refer to Supplemental Table 1 online). Kanamycin-positive primary transformants were analyzed for reduced *Exo70A1* expression by RNA gel blot analysis as previously described (Stone et al., 1999). These lines were also analyzed for pollen adhesion, pollen tube growth, and seed set as described previously (Stone et al., 1999). The R2 and R3 *Exo70A1* RNAi Westar lines were analyzed in the T2 generation as well, and they displayed the same pollen rejection traits observed in the T1 plants. Pollinations for aniline blue staining were performed as previously described (Stone et al., 1999). The aniline blue fluorescence was captured as gray-scale images, colored green, and overlaid with the red autofluorescence obtained from pollen. For the hydration experiments, pedicels of newly opened flowers were immersed in water and pollen grains (6 to 10) were added on the top of the stigma. Pollen hydration was tracked using a LeicaMZ16 stereomicroscope, and images were captured from a polar view for 10 min using a Leica camera with the LAS v.2.5.OR1 program. These images were processed through ImageJ to measure the principal diameter of the pollen grains during the hydration process.

For the *RFP:Exo70A1* W1 lines, the *B. napus Exo70A1* open reading frame fused to RFP was subcloned behind a binary vector containing the SLR1 promoter and transformed into W1 plants using *Agrobacterium tumefaciens*–mediated transformation. Transgenic lines were screened and analyzed as described above. Expression was analyzed by RT-PCR using primers to specifically detect the *RFP:Exo70A1* mRNA, and actin was used as a positive control. For RT-PCR, total RNA was isolated from the stigmas from various transgenic and control plants and used to synthesize cDNA through oligo(dT)-mediated reverse transcription. From this, 1 μL of cDNA was used for PCR using gene-specific primers (see Supplemental Table 1 online). RT-PCR products were visualized using ethidium bromide. Confocal microscopy was also used to examine the localization pattern of RFP:Exo70A1, but the expression levels were not high enough to visualize the RFP fluorescence in the dense *Brassica* stigmatic papillae. The same construct gave successful confocal results in the more transparent *Arabidopsis* stigmatic papillae (see below).

For protein gel blotting using anti-RFP antibodies, stigmatic proteins were extracted from either unpollinated or pollinated pistils from the transgenic *RFP:Exo70A1* W1 S1 line, and pollinations were performed with either self-incompatible W1 pollen or compatible Westar pollen. Protein extracts were fractionated on a 7% SDS-PAGE gel and probed with anti-RFP antibodies.

Arabidopsis exo70A1 T-DNA Insertion Lines

Two SALK T-DNA insertion lines for *Exo70A1* were analyzed as shown in Supplemental Figures 3A to 3D online. These lines were previously reported by Synek et al. (2006) as having defects in the elongation of stigmatic papillae in flowers from 8-week-old plants. We observed that the stigmas showed variability in stigmatic papillar elongation at flower bud opening (see Supplemental Figures 4D and 4E online) and found that the *exo70A1* mutants would produce more fully elongated stigmatic papillae when the plants were misted daily. For the pollen hydration studies, stage 12 flowers from Col-0 plants were emasculated and covered with plastic wrap overnight to allow flower development to stage 13 (Smith et al., 1990). For the *exo70A1-1* plants, the largest buds (which would roughly represent stage 12 flowers) were emasculated and left overnight, and stigmas with elongated papillae were used for the hydration studies. Since the *exo70A1-1* plants are sterile, pistils from open flowers were also tested, yielding the same results.

Pistils were excised and mounted on a microscope slide using double-sided tape. An individual Col-0 pollen grain was placed on a stigmatic papilla using a Sisikiyou Designs 7600 micromanipulator. The pollen grain was then monitored using an inverted Olympus IX51 microscope with a ×10 objective, and images were acquired with a CCD camera (Roper Scientific) using ImageMaster. Pollinations were conducted under low-humidity conditions (relative humidity below 35%, as monitored with a digital hygrometer [VWR 35519-044]; $n = 11$).

Arabidopsis RFP:Exo70A1 Transgenic Lines

The $SLR1_{pro}$*RFP:Exo70A1* (*B. napus Exo70A1*) construct was used to transform heterozygous *Exo70A1/exo70A1-1 Arabidopsis* plants using the floral dip method (Clough and Bent, 1998). The segregating T0 seeds were selected on kanamycin and genotyped to isolate wild-type and *exo70 A1-1* mutant plants expressing *RFP:Exo70A1*. Two of the strongest lines, S4 and S14, were used to analyze the rescue of pollen adherence, pollen tube growth, and seed set following pollination with wild-type Col-0 pollen. Controlled pollinations were performed using pistils from Col-0, *exo70A1-1*, and *RFP:Exo70A1/exo70A1-1* plants to assess pollen adhesion, pollen tube growth, and seed set using Col-0 pollen. Stage 12 flowers were emasculated and covered with plastic wrap for 24 h, hand-pollinated with Col-0 pollen, and rewrapped again in plastic wrap for 24 h. For pollen adhesion and pollen tube growth studies, the pistils were then stained with aniline blue and observed with an epifluorescence microscope. For seed production, the coverings were removed, and the siliques were allowed to mature (10 to 12 d). Mature siliques were opened, and seeds/fertilized ovules were counted.

Confocal Microscopy

For the staining of *Arabidopsis* Col-0 and *exo70A1-1* pistils with FM1-43, stage 11 flowers from Col-0 and *exo70A1-1* plants were emasculated and covered with a plastic wrap for a 16-h period. The prepared pistils were mounted in half-strength Murashige and Skoog buffer containing FM1-43 (1 μg/μL) followed by confocal imaging using an LSM510 (Carl Zeiss) Zeiss 63X Plan-Apochromat oil-immersion objective.

For the confocal microscopy of wild-type and *exo70A1-1* plants expressing *RFP:Exo70A1*, the flowers were emasculated similarly, left for various lengths of time, mounted in Vectashield mounting medium (Vector Laboratories; H-1000), and observed using an LSM510 (Carl Zeiss) 40× oil-immersion objective. For postpollination experiments, stigmas were pollinated with Col-0 pollen prior to mounting and viewing. *Arabidopsis* GFP marker lines for the Golgi, vacuole, and plasma

membrane (Cutler et al., 2000; Saint-Jore et al., 2002) were crossed with the *RFP:Exo70A1* S14/Col-0 plants to obtain lines with both the GFP-marked compartment and *RFP:Exo70A1*.

Arabidopsis Exo70A1$_{pro}$GUS Analysis

A 2.5-kb sequence upstream of the *Arabidopsis Exo70A1* coding region was amplified from *Arabidopsis* genomic DNA and placed in front of the GUS coding sequence of the plant expression vector pCAMBIA1391Z. This construct was mobilized into *Agrobacterium* GV3101, followed by *Agrobacterium*-mediated transformation of wild-type Col-0 plants using the floral dip method (Clough and Bent, 1998). The hygromycin-resistant transformants were screened for GUS expression at various growth stages. In brief, tissues were infiltrated with GUS buffer for 20 min, followed by incubation for 1 h at 37°C. The samples were then washed in 100% ethanol, mounted with a 8:2:1 mixture of chloral hydrate:water: glycerol, and viewed under a LeicaMZ16 stereomicroscope.

Tobacco BY-2 Cell Transformation and Epifluorescence Microscopy

Biolistic-mediated transformation of log-phase BY-2 suspension-cultured cells was performed as described (Stone et al., 2003; Samuel et al., 2008). Single transformations were performed with a total of 10 μg of purified plasmid DNA, and cobombardments used 10 to 15 μg of total plasmids combined (with equal quantities of each plasmid). Following transformations, BY-2 cells were left in the dark and then harvested at 20 h postbombardment, fixed, and either visualized directly for fluorescent proteins or treated with antibodies to detect epitope-tagged proteins as described (Stone et al., 2003; Samuel et al., 2008). Constructs used are shown in Figure 8. Full-length ARC1 was fused to myc or GFP, while full-length *Exo70A1* was fused to RFP or GFP, and GST:SRK$_{A14}$ was used as previously described (Stone et al., 2003). Full-length RPT2A was amplified from *Arabidopsis* leaf cDNA and cloned as an RFP fusion. RFP:RPT2A is a proteasomal ATPase subunit. The ER marker, Concanavalin A-594 conjugate (Molecular Probes), was used at a final concentration of 100 μg/mL for the colocalization experiments. The Syp21 and Syp42 marker plasmids are from Uemura et al. (2004).

Accession Numbers

Sequence data from this article can be found in the Arabidopsis Genome Initiative or GenBank/EMBL databases under the following accession numbers: *B. napus* Exo70A1 (GQ503256) and *Arabidopsis* Exo70A1 (NM_001125690; At5g03540).

Author Contributions

M.A.S., Y.T.C., K.E.H., and D.R.G. conceived and designed the experiments. M.A.S., Y.T.C., K.E.H., M.G.B., and S.L.S. performed the experiments. M.A.S., Y.T.C., K.E.H., and D.R.G. analyzed the data and wrote the manuscript.

Supplemental Data

The following materials are available in the online version of this article.

Supplemental Figure 1. Amino Acid Alignments of *Brassica napus* Exo70A1 to Different Mmembers of the *Arabidopsis* Exo70 Gene Family.

Supplemental Figure 2. RFP:Exo70A1 Protein Levels Following Self-Incompatible W1 and Compatible Westar Pollinations.

Supplemental Figure 3. *Arabidopsis exo70A1* T-DNA Insertional Lines.

Supplemental Figure 4. Unpollinated and Pollinated Stigmas from *Arabidopsis* Col-0, the *exo70A1-1* Mutant, and the Rescued *exo70A1-1* Mutant Line Expressing *RFP:Exo70A1*.

Supplemental Figure 5. Transgenic *Arabidopsis* Lines Expressing Different GFP Marker Proteins in the Stigma.

Supplemental Table 1. Primers Used in This Study.

ACKNOWLEDGMENTS

We thank He Sun for technical assistance, Henry Hong for confocal microscopy assistance, and Melanie Woodin for assistance with the micromanipulator pollinations. We also thank Martin Trick for the SLR1 promoter, Sean Cutler for the GFP:δ-TIP and GFP:PIP2A lines, Chris Hawes for the ST-GFP *Arabidopsis* line, Masa H. Sato for the GFP:Syp21 and GFP:Syp42 plasmids, and Robert Mullen for the BY-2 expression marker constructs, anti-RFP antibodies, and helpful discussions. Finally, we thank Erik Nielsen and Ed Newbigin for constructive comments on the manuscript. This work was supported by grants from the Natural Sciences and Engineering Research Council of Canada and a Canada Research Chair to D.R.G.

Received July 2, 2009; revised September 3, 2009; accepted September 11, 2009; published September 29, 2009.

REFERENCES

Barile, M., Pisitkun, T., Yu, M.J., Chou, C.L., Verbalis, M.J., Shen, R.F., and Knepper, M.A. (2005). Large scale protein identification in intracellular aquaporin-2 vesicles from renal inner medullary collecting duct. Mol. Cell. Proteomics **4:** 1095–1106.

Boevink, P., Oparka, K., Santa Cruz, S., Martin, B., Betteridge, A., and Hawes, C. (1998). Stacks on tracks: The plant Golgi apparatus traffics on an actin/ER network. Plant J. **15:** 441–447.

Boyd, C., Hughes, T., Pypaert, M., and Novick, P. (2004). Vesicles carry most exocyst subunits to exocytic sites marked by the remaining two subunits, Sec3p and Exo70p. J. Cell Biol. **167:** 889–901.

Chong, Y.T., Gidda, S.K., Sanford, C., Parkinson, J., Mullen, R.T., and Goring, D.R. (2009). Characterisation of the *Arabidopsis* exocyst complex gene families by phylogenetic, expression profiling, and subcellular localisation studies. New Phytol., in press.

Clough, S.J., and Bent, A.F. (1998). Floral dip: A simplified method for Agrobacterium-mediated transformation of *Arabidopsis thaliana.* Plant J. **16:** 735–743.

Cole, R.A., Synek, L., Zarsky, V., and Fowler, J.E. (2005). SEC8, a subunit of the putative Arabidopsis exocyst complex, facilitates pollen germination and competitive pollen tube growth. Plant Physiol. **138:** 2005–2018.

Cutler, S.R., Ehrhardt, D.W., Griffitts, J.S., and Somerville, C.R. (2000). Random GFP:cDNA fusions enable visualization of subcellular structures in cells of Arabidopsis at a high frequency. Proc. Natl. Acad. Sci. USA **97:** 3718–3723.

Dickinson, H. (1995). Dry stigmas, water and self-incompatibility in *Brassica.* Sex. Plant Reprod. **8:** 1–10.

Doughty, J., Dixon, S., Hiscock, S.J., Willis, A.C., Parkin, I.A., and Dickinson, H.G. (1998). PCP-A1, a defensin-like *Brassica* pollen coat protein that binds the S locus glycoprotein, is the product of gametophytic gene expression. Plant Cell **10:** 1333–1347.

EauClaire, S., and Guo, W. (2003). Conservation and specialization. The role of the exocyst in neuronal exocytosis. Neuron **37:** 369–370.

Edlund, A.F., Swanson, R., and Preuss, D. (2004). Pollen and stigma

structure and function: The role of diversity in pollination. Plant Cell **16** (suppl.): S84–S97.

Elleman, C.J., and Dickinson, H.G. (1990). The role of the exine coating in pollen-stigma interactions in *Brassica oleracea.* New Phytol. **114:** 511–518.

Elleman, C.J., and Dickinson, H.G. (1996). Identification of pollen components regulating pollination-specific responses in the stigmatic papillae of *Brassica oleracea.* New Phytol. **133:** 197–205.

Fiebig, A., Mayfield, J.A., Miley, N.L., Chau, S., Fischer, R.L., and Preuss, D. (2000). Alterations in *CER6*, a gene identical to *CUT1*, differentially affect long-chain lipid content on the surface of pollen and stems. Plant Cell **12:** 2001–2008.

Fobis-Loisy, I., Chambrier, P., and Gaude, T. (2007). Genetic transformation of *Arabidopsis lyrata*: Specific expression of the green fluorescent protein (GFP) in pistil tissues. Plant Cell Rep. **26:** 745–753.

Folsch, H., Pypaert, M., Maday, S., Pelletier, L., and Mellman, I. (2003). The AP-1A and AP-1B clathrin adaptor complexes define biochemically and functionally distinct membrane domains. J. Cell Biol. **163:** 351–362.

Franklin, T.M., Oldknow, J., and Trick, M. (1996). SLR1 function is dispensable for both self-incompatible rejection and self-compatible pollination processes in *Brassica.* Sex. Plant Reprod. **9:** 203–208.

Goring, D.R., and Walker, J.C. (2004). Plant sciences. Self-rejection–a new kinase connection. Science **303:** 1474–1475.

Gu, T., Mazzurco, M., Sulaman, W., Matias, D.D., and Goring, D.R. (1998). Binding of an arm repeat protein to the kinase domain of the S-locus receptor kinase. Proc. Natl. Acad. Sci. USA **95:** 382–387.

Guo, W., Roth, D., Walch-Solimena, C., and Novick, P. (1999). The exocyst is an effector for Sec4p, targeting secretory vesicles to sites of exocytosis. EMBO J. **18:** 1071–1080.

Hala, M., Cole, R., Synek, L., Drdova, E., Pecenkova, T., Nordheim, A., Lamkemeyer, T., Madlung, J., Hochholdinger, F., Fowler, J.E., and Zarsky, V. (2008). An exocyst complex functions in plant cell growth in *Arabidopsis* and tobacco. Plant Cell **20:** 1330–1345.

He, B., and Guo, W. (2009). The exocyst complex in polarized exocytosis. Curr. Opin. Cell Biol. **21:** 537–542.

Heslop-Harrison, J. (1981). Stigma characteristics and angiosperm taxonomy. Nord. J. Bot. **1:** 401–420.

Hiscock, S.J., and Allen, A.M. (2008). Diverse cell signalling pathways regulate pollen-stigma interactions: The search for consensus. New Phytol. **179:** 286–317.

Hiscock, S.J., and McInnis, S.M. (2003). Pollen recognition and rejection during the sporophytic self-incompatibility response: *Brassica* and beyond. Trends Plant Sci. **8:** 606–613.

Hsu, S.C., TerBush, D., Abraham, M., and Guo, W. (2004). The exocyst complex in polarized exocytosis. Int. Rev. Cytol. **233:** 243–265.

Hulskamp, M., Kopczak, S.D., Horejsi, T.F., Kihl, B.K., and Pruitt, R. E. (1995). Identification of genes required for pollen-stigma recognition in *Arabidopsis thaliana.* Plant J. **8:** 703–714.

Inoue, M., Chang, L., Hwang, J., Chiang, S.H., and Saltiel, A.R. (2003). The exocyst complex is required for targeting of Glut4 to the plasma membrane by insulin. Nature **422:** 629–633.

Inoue, M., Chiang, S.H., Chang, L., Chen, X.W., and Saltiel, A.R. (2006). Compartmentalization of the exocyst complex in lipid rafts controls Glut4 vesicle tethering. Mol. Biol. Cell **17:** 2303–2311.

Iwano, M., Shiba, H., Matoba, K., Miwa, T., Funato, M., Entani, T., Nakayama, P., Shimosato, H., Takaoka, A., Isogai, A., and Takayama, S. (2007). Actin dynamics in papilla cells of *Brassica rapa* during self- and cross-pollination. Plant Physiol. **144:** 72–81.

Kachroo, A., Schopfer, C.R., Nasrallah, M.E., and Nasrallah, J.B. (2001). Allele-specific receptor-ligand interactions in *Brassica* self-incompatibility. Science **293:** 1824–1826.

Kakita, M., Murase, K., Iwano, M., Matsumoto, T., Watanabe, M., Shiba, H., Isogai, A., and Takayama, S. (2007). Two distinct forms of M-locus protein kinase localize to the plasma membrane and interact directly with S-locus receptor kinase to transduce self-incompatibility signaling in *Brassica rapa.* Plant Cell **19:** 3961–3973.

Lipschutz, J.H., and Mostov, K.E. (2002). Exocytosis: The many masters of the exocyst. Curr. Biol. **12:** R212–R214.

Lolle, S.J., and Cheung, A.Y. (1993). Promiscuous germination and growth of wildtype pollen from *Arabidopsis* and related species on the shoot of the *Arabidopsis* mutant, *fiddlehead.* Dev. Biol. **155:** 250–258.

Luu, D.T., Marty-Mazars, D., Trick, M., Dumas, C., and Heizmann, P. (1999). Pollen-stigma adhesion in *Brassica* spp involves SLG and SLR1 glycoproteins. Plant Cell **11:** 251–262.

Matern, H.T., Yeaman, C., Nelson, W.J., and Scheller, R.H. (2001). The Sec6/8 complex in mammalian cells: Characterization of mammalian Sec3, subunit interactions, and expression of subunits in polarized cells. Proc. Natl. Acad. Sci. USA **98:** 9648–9653.

Mayfield, J.A., and Preuss, D. (2000). Rapid initiation of *Arabidopsis* pollination requires the oleosin-domain protein GRP17. Nat. Cell Biol. **2:** 128–130.

Munson, M., and Novick, P. (2006). The exocyst defrocked, a framework of rods revealed. Nat. Struct. Mol. Biol. **13:** 577–581.

Murase, K., Shiba, H., Iwano, M., Che, F.S., Watanabe, M., Isogai, A., and Takayama, S. (2004). A membrane-anchored protein kinase involved in *Brassica* self-incompatibility signaling. Science **303:** 1516–1519.

Oztan, A., Silvis, M., Weisz, O.A., Bradbury, N.A., Hsu, S.C., Goldenring, J.R., Yeaman, C., and Apodaca, G. (2007). Exocyst requirement for endocytic traffic directed toward the apical and basolateral poles of polarized MDCK cells. Mol. Biol. Cell **18:** 3978–3992.

Roberts, I.N., Harrod, G., and Dickinson, H.G. (1984). Pollen-stigma interactions in *Brassica oleracea*. I. Ultrastructure and physiology of the stigmatic papillar cells. J. Cell Sci. **66:** 241–253.

Saint-Jore, C.M., Evins, J., Batoko, H., Brandizzi, F., Moore, I., and Hawes, C. (2002). Redistribution of membrane proteins between the Golgi apparatus and endoplasmic reticulum in plants is reversible and not dependent on cytoskeletal networks. Plant J. **29:** 661–678.

Samaj, J., Read, N.D., Volkmann, D., Menzel, D., and Baluska, F. (2005). The endocytic network in plants. Trends Cell Biol. **15:** 425–433.

Samuel, M.A., and Ellis, B.E. (2002). Double jeopardy: Both overexpression and suppression of a redox-activated plant mitogen-activated protein kinase render tobacco plants ozone sensitive. Plant Cell **14:** 2059–2069.

Samuel, M.A., Mudgil, Y., Salt, J.N., Delmas, F., Ramachandran, S., Chilelli, A., and Goring, D.R. (2008). Interactions between the S-domain receptor kinases and AtPUB-ARM E3 ubiquitin ligases suggest a conserved signaling pathway in Arabidopsis. Plant Physiol. **147:** 2084–2095.

Sanderfoot, A.A., Kovaleva, V., Bassham, D.C., and Raikhel, N.V. (2001). Interactions between syntaxins identify at least five SNARE complexes within the Golgi/prevacuolar system of the Arabidopsis cell. Mol. Biol. Cell **12:** 3733–3743.

Schopfer, C.R., Nasrallah, M.E., and Nasrallah, J.B. (1999). The male determinant of self-incompatibility in *Brassica.* Science **286:** 1697–1700.

Schranz, M.E., Song, B.H., Windsor, A.J., and Mitchell-Olds, T. (2007). Comparative genomics in the Brassicaceae: a family-wide perspective. Curr. Opin. Plant Biol. **10:** 168–175.

Silva, N.F., Stone, S.L., Christie, L.N., Sulaman, W., Nazarian, K.A., Burnett, L.A., Arnoldo, M.A., Rothstein, S.J., and Goring, D.R. (2001). Expression of the S receptor kinase in self-compatible *Brassica napus* cv. Westar leads to the allele-specific rejection of self-incompatible *Brassica napus* pollen. Mol. Genet. Genomics **265:** 552–559.

Smyth, D.R., Bowman, J.L., and Meyerowitz, E.M. (1990). Early flower development in *Arabidopsis*. Plant Cell **2:** 755–767.

Stone, S.L., Anderson, E.M., Mullen, R.T., and Goring, D.R. (2003). ARC1 is an E3 ubiquitin ligase and promotes the ubiquitination of proteins during the rejection of self-incompatible *Brassica* pollen. Plant Cell **15:** 885–898.

Stone, S.L., Arnoldo, M., and Goring, D.R. (1999). A breakdown of *Brassica* self-incompatibility in ARC1 antisense transgenic plants. Science **286:** 1729–1731.

Swanson, R., Edlund, A.F., and Preuss, D. (2004). Species specificity in pollen-pistil interactions. Annu. Rev. Genet. **38:** 793–818.

Synek, L., Schlager, N., Elias, M., Quentin, M., Hauser, M.T., and Zarsky, V. (2006). AtEXO70A1, a member of a family of putative exocyst subunits specifically expanded in land plants, is important for polar growth and plant development. Plant J. **48:** 54–72.

Takasaki, T., Hatakeyama, K., Suzuki, G., Watanabe, M., Isogai, A., and Hinata, K. (2000). The S receptor kinase determines self-incompatibility in *Brassica* stigma. Nature **403:** 913–916.

Takayama, S., and Isogai, A. (2005). Self-incompatibility in plants. Annu. Rev. Plant Biol. **56:** 467–489.

Takayama, S., Shiba, H., Iwano, M., Asano, K., Hara, M., Che, F.S., Watanabe, M., Hinata, K., and Isogai, A. (2000a). Isolation and characterization of pollen coat proteins of *Brassica campestris* that interact with *S* locus-related glycoprotein 1 involved in pollen-stigma adhesion. Proc. Natl. Acad. Sci. USA **97:** 3765–3770.

Takayama, S., Shiba, H., Iwano, M., Shimosato, H., Che, F.S., Kai, N., Watanabe, M., Suzuki, G., Hinata, K., and Isogai, A. (2000b). The pollen determinant of self-incompatibility in *Brassica campestris*. Proc. Natl. Acad. Sci. USA **97:** 1920–1925.

Takayama, S., Shimosato, H., Shiba, H., Funato, M., Che, F.S., Watanabe, M., Iwano, M., and Isogai, A. (2001). Direct ligand-receptor complex interaction controls *Brassica* self-incompatibility. Nature **413:** 534–538.

Uemura, T., Ueda, T., Ohniwa, R.L., Nakano, A., Takeyasu, K., and Sato, M.H. (2004). Systematic analysis of SNARE molecules in Arabidopsis: Dissection of the post-Golgi network in plant cells. Cell Struct. Funct. **29:** 49–65.

Wen, T.J., Hochholdinger, F., Sauer, M., Bruce, W., and Schnable, P. S. (2005). The roothairless1 gene of maize encodes a homolog of sec3, which is involved in polar exocytosis. Plant Physiol. **138:** 1637–1643.

Yu, K., Schafer, U., Glavin, T.L., Goring, D.R., and Rothstein, S.J. (1996). Molecular characterization of the S locus in two self-incompatible *Brassica napus* lines. Plant Cell **8:** 2369–2380.

Zárský, V., Cvrčková, F., Potocký, M., and Hála, M. (2009). Exocytosis and cell polarity in plants - Exocyst and recycling domains. New Phytol. **183:** 255–272.

Zinkl, G.M., Zwiebel, B.I., Grier, D.G., and Preuss, D. (1999). Pollen-stigma adhesion in *Arabidopsis*: A species-specific interaction mediated by lipophilic molecules in the pollen exine. Development **126:** 5431–5440.